

CHAPTER 18

COMPLEX TERNARY SYSTEMS

Having examined the structural units from which ternary phase diagrams are built, it remains to consider the ways in which these may be assembled into the relatively complex diagrams that are characteristic of the majority of ternary alloy systems. Portions of many three-component metal systems have been examined in the laboratory, and phase diagrams have been published, but in very few cases can it be said that the ternary diagram has been even approximately established in all its parts. Indeed, only small areas of the diagram adjacent to alloy compositions of immediate technical interest have been investigated in the majority of ternary systems. This is a pronounced handicap in the interpretation of such diagrams, where, as often happens, the composition ranges of some of the phases which participate in reactions in the explored areas themselves lie in unexplored areas. For this reason it is of more than academic interest to be able to speculate intelligently concerning constructions that are possible in regions of diagrams relative to which only fragmentary information is available. Practice in the synthesis of ternary diagrams from real or assumed data is useful in developing skill in this type of reasoning.

Review of Structural Units

Before proceeding with the assembly of whole diagrams, the structural units that have been discussed in preceding chapters will be summarized in review (see Fig. 18-1). *One-phase equilibria* are represented by spaces of any shape, bounded by surfaces of the two-phase regions and, hence, cannot be represented by any characteristic structural unit.

Two-phase equilibrium is always represented by spaces having two conjugate surfaces that are joined at every point by tie-lines connecting the compositions of the conjugate phases (Fig. 18-1a). Where congruent transformation occurs between the two phases, the bounding surfaces of the two-phase region meet at a single point as at the melting point of a pure component (Fig. 18-1b) or at the congruent melting point of an

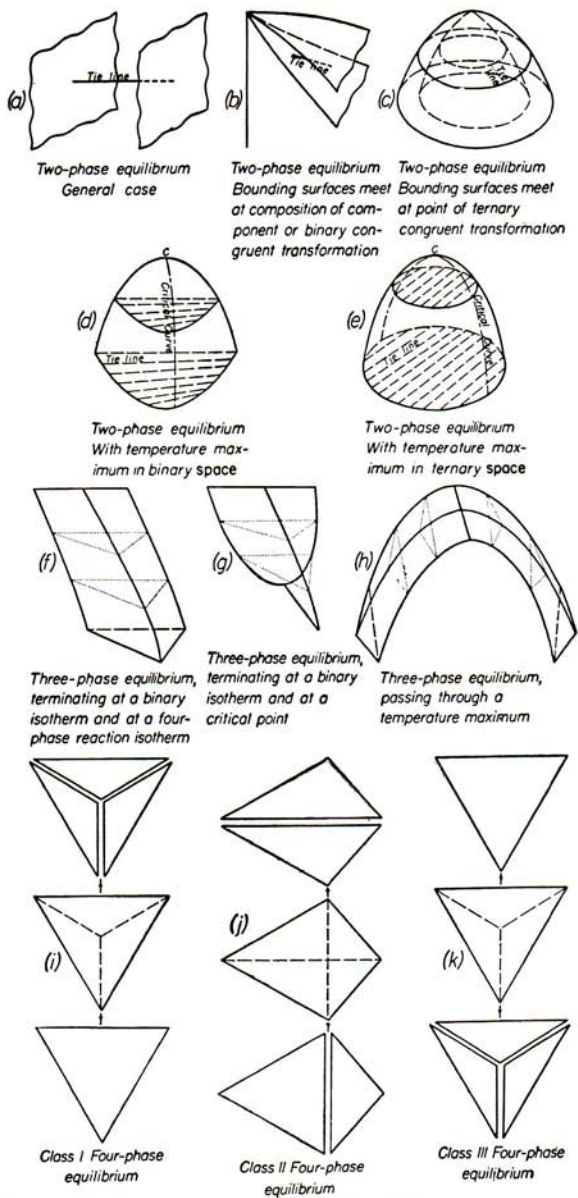


FIG. 18-1. Elements of construction of ternary temperature-composition diagrams.

intermediate phase (Fig. 18-1c). Such points are always at temperature maxima or minima.

A region of two-phase equilibrium may also terminate in a critical point which may lie in one of the binary faces of the space diagram (Fig. 18-1d) or may lie within the ternary space of the diagram (Fig. 18-1e). The critical point itself represents the highest or lowest temperature at which the two phases may coexist and is, therefore, a maximum or minimum point. There is also a critical curve, which connects the points on successive isotherms at which the tie-lines are reduced to zero length.

Three-phase equilibrium is represented by a trio of conjugate curves everywhere connected by tie-triangles. Such a region may terminate in a horizontal line at a temperature maximum or minimum at a binary three-phase isotherm (Fig. 18-1f) or in space (Fig. 18-1g) or at a quasi-binary section (Fig. 18-1h). It may also terminate in a final tie-triangle at a temperature minimum or maximum where a four-phase reaction plane is intersected (Fig. 18-1f).

Four-phase equilibrium may be represented by any of three distinct constructions. In class I four-phase equilibrium three three-phase regions involving a total of four phases approach a triangular reaction plane from higher temperature, one phase vanishes, and a single three-phase region descends to lower temperature (Fig. 18-1i). Eighteen combinations of four phases that may conceivably join in class I reaction are listed in Table 4. Among these, reaction *Ih* will be recognized as the ternary eutectic, *Io* as the ternary eutectoid, and *Ik* as a version of the ternary monotectic which was discussed at the end of Chap. 14. No names have been applied to any but the ternary eutectic and ternary eutectoid.

Class II equilibrium (Fig. 18-1j) occurs when four phases represented in two three-phase regions that have two phases in common approach from higher temperature and join along a common tie-line to form a trapezium at the four corners of which the compositions of the four phases are designated. Reaction is represented by the division of the trapezium into two tie-triangles having the opposite two phases in common, the corresponding three-phase regions proceeding to lower temperature. A list of 21 conceivable class II reactions is given in Table 4. Reaction *IIp* was employed as a typical example in Chap. 15. Several of the others are encountered in existing phase diagrams. None has a special name; it is not correct to refer to any class II reaction as a ternary peritectic reaction.

The third form of four-phase equilibrium, class III, is represented as in Fig. 18-1k. One three-phase region descends from higher temperature and splits into three three-phase regions isothermally at a triangular reaction plane where the fourth phase first makes its appearance. This is the peritectic type of ternary reaction. Eighteen combinations of phases

that could conceivably partake in class III four-phase reaction are listed in Table 4. Reaction IIIo, in which the γ phase is an intermediate that melts incongruently, is probably the most common in ternary phase diagrams. No special names have been assigned to any of these reactions, but the use of the name "ternary peritectic" for IIIo and "ternary peritectoid" for IIIr seems logical.

TABLE 4. TYPES OF TERNARY FOUR-PHASE EQUILIBRIA

| Class I | Class II | Class III |
|---|--|---|
| Ia. $G \rightarrow L_I + L_{II} + L_{III}$ | IIa. $G + L_I \rightarrow L_{II} + L_{III}$ | IIIa. $G + L_I + L_{II} \rightarrow L_{III}$ |
| Ib. $G \rightarrow L_I + L_{II} + \alpha$ | IIb. $G + L_I \rightarrow L_{II} + \alpha$ | IIIb. $G + L_I + L_{II} \rightarrow \alpha$ |
| Ic. $G \rightarrow L_I + \alpha + \beta$ | IIc. $G + L_I \rightarrow \alpha + \beta$ | IIIc. $G + L_I + \alpha \rightarrow L_{II}$ |
| Id. $G \rightarrow \alpha + \beta + \gamma$ | II d. $G + \alpha \rightarrow L_I + L_{II}$ | III d. $G + L_I + \alpha \rightarrow \beta$ |
| Ie. $L_I \rightarrow G + L_{II} + L_{III}$ | IIe. $G + \alpha \rightarrow L_I + \beta$ | IIIe. $G + \alpha + \beta \rightarrow L_I$ |
| If. $L_I \rightarrow G + L_{II} + \alpha$ | II f. $G + \alpha \rightarrow \beta + \gamma$ | III f. $G + \alpha + \beta \rightarrow \gamma$ |
| Ig. $L_I \rightarrow G + \alpha + \beta$ | IIg. $L_I + L_{II} \rightarrow L_{III} + L_{IV}$ | IIIg. $L_I + L_{II} + L_{III} \rightarrow G$ |
| Ih. $L_I \rightarrow \alpha + \beta + \gamma$ | IIh. $L_I + L_{II} \rightarrow L_{III} + \alpha$ | IIIh. $L_I + L_{II} + L_{III} \rightarrow L_{IV}$ |
| Ii. $L_I \rightarrow L_{II} + L_{III} + L_{IV}$ | IIi. $L_I + L_{II} \rightarrow \alpha + \beta$ | IIIi. $L_I + L_{II} + L_{III} \rightarrow \alpha$ |
| Ij. $L_I \rightarrow L_{II} + L_{III} + \alpha$ | IIj. $L_I + L_{II} \rightarrow G + L_{III}$ | IIIj. $L_I + L_{II} + \alpha \rightarrow G$ |
| Ik. $L_I \rightarrow L_{II} + \alpha + \beta$ | IIk. $L_I + L_{II} \rightarrow G + \alpha$ | IIIk. $L_I + L_{II} + \alpha \rightarrow L_{III}$ |
| Il. $\alpha \rightarrow G + L_I + L_{II}$ | IIl. $L_I + \alpha \rightarrow G + L_{II}$ | IIIl. $L_I + L_{II} + \alpha \rightarrow \beta$ |
| I m. $\alpha \rightarrow G + L_I + \beta$ | II m. $L_I + \alpha \rightarrow G + \beta$ | III m. $L_I + \alpha + \beta \rightarrow G$ |
| Io. $\alpha \rightarrow G + \beta + \gamma$ | II n. $L_I + \alpha \rightarrow L_{II} + L_{III}$ | III n. $L_I + \alpha + \beta \rightarrow L_{II}$ |
| I p. $\alpha \rightarrow \beta + \gamma + \delta$ | II o. $L_I + \alpha \rightarrow L_{II} + \beta$ | III o. $L_I + \alpha + \beta \rightarrow \gamma$ |
| Iq. $\alpha \rightarrow L_I + L_{II} + L_{III}$ | II p. $L_I + \alpha \rightarrow \beta + \gamma$ | III p. $\alpha + \beta + \gamma \rightarrow G$ |
| I r. $\alpha \rightarrow L_I + L_{II} + \beta$ | II q. $\alpha + \beta \rightarrow G + L_I$ | III q. $\alpha + \beta + \gamma \rightarrow L_I$ |
| | II r. $\alpha + \beta \rightarrow G + \gamma$ | III r. $\alpha + \beta + \gamma \rightarrow \delta$ |
| | II s. $\alpha + \beta \rightarrow L_I + L_{II}$ | |
| | II t. $\alpha + \beta \rightarrow L_I + \gamma$ | |
| | II u. $\alpha + \beta \rightarrow \gamma + \delta$ | |

Assembly of the Ternary Diagram

The assembly of the structural units into a complete diagram involving a variety of forms, such as the example of Fig. 18-2, is assisted by observing the following rules:

1. One-phase regions may meet each other only at single points, which are also temperature maxima or minima.
2. One-phase regions are elsewhere separated from each other by two-phase regions representing the two phases concerned; thus, the bounding surfaces of one-phase regions are always boundaries of two-phase regions.
3. One-phase fields touch three-phase regions only along lines which are generally nonisothermal.
4. One-phase regions touch four-phase reaction planes only at single points.

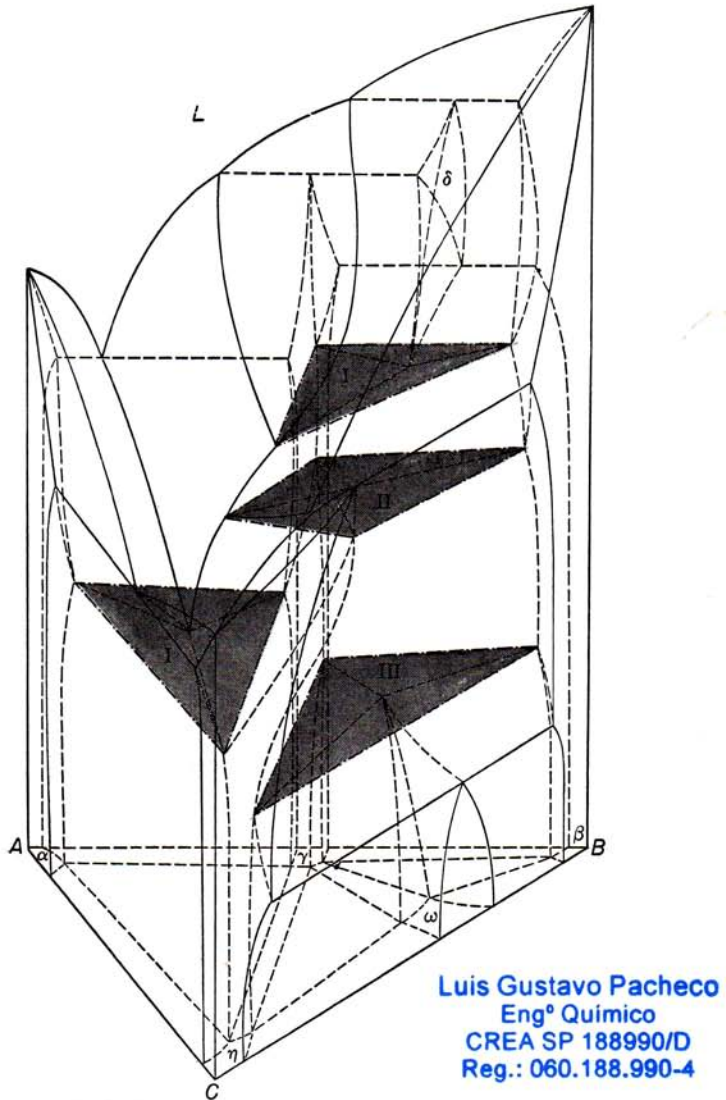


FIG. 18-2. A hypothetical ternary temperature-composition diagram involving all three classes of four-phase equilibrium.

5. *Two-phase* regions touch each other only along lines which, in general, are nonisothermal.

6. *Two-phase* regions are elsewhere separated by one- and three-phase regions by whose bounding surfaces they are enclosed.

7. *Two-phase* regions meet three-phase regions upon "ruled" bounding surfaces generated by the limiting tie-lines.

8. *Two-phase* regions touch four-phase reaction planes along single isothermal lines, which are limiting tie-lines.

9. *Three-phase* regions meet each other nowhere except at the four-phase reaction isotherms.

10. *Three-phase* regions are elsewhere separated and bounded by two-phase regions involving those two phases which are held in common by the neighboring three-phase regions.

These conditions can be summarized as follows: *A field of the phase diagram, representing equilibrium among a given number of phases, can be bounded only by regions representing equilibria among one more or one less than the given number of phases.* This statement is quite general; it applies

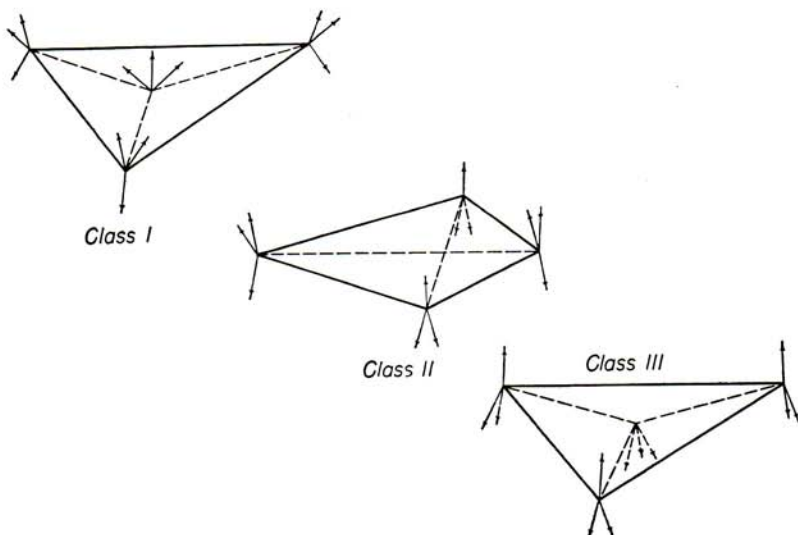


FIG. 18-3

to binary systems and to those of four and more components as well as to the ternary systems. In applying this rule it is admissible, and proper to consider the univariant equilibrium isotherms as "regions."

In constructing a diagram such as that shown in Fig. 18-2, it is well to remember that each four-phase isotherm must be associated with four three-phase regions, six two-phase regions, and four one-phase regions. This arrangement requires that three lines (no more and no less) shall meet the reaction isotherm at each of the four points at which it touches the one-phase regions. Twelve lines in all are attached to each four-phase isotherm (see Fig. 18-3). Two four-phase equilibria that have three phases in common may be connected by a three-phase region involving the three phases concerned. More than one three-phase region may never

run between any pair of four-phase reaction isotherms unless they have all four phases in common.

Attention is directed again to the rule of construction illustrated in Fig. 13-7, which states that in the isothermal section through the ternary space diagram, the boundaries of a one-phase region where it meets a three-phase region must be so drawn that if projected, they would *both* extend into two-phase regions or *both* extend into the three-phase region but *never* one into a two-phase region while the other projects into the three-phase region or either or both into the one-phase region. The structure of isotherms may be further verified by the use of the rule, described at the end of the previous chapter, which relates the number of three-phase equilibria n to the number of binary b and ternary t intermediate phases in the system $n = b + 2t + 1$.

The division of the ternary diagram into independent sections by quasi-binary sections greatly simplifies the structure of the diagram, because each section may then be treated separately. True quasi-binary sections are by no means so common, however, among "metal" systems as they are among "chemical" systems, where many very stable compounds exist. It is usually unwise to assume the existence of a quasi-binary system unless there is definite evidence of its reality.

Ternary Models for Practice

At the end of this chapter a group of practice problems is given. The construction of the "problem diagrams" with due observance of the

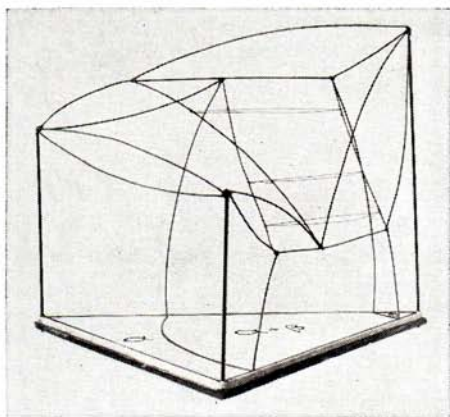


FIG. 18-4. Wire model of the space diagram illustrated in Fig. 13-18.

foregoing rules and generalizations should be of considerable assistance in developing a "feel for ternary diagrams." Many students of the subject find it helpful also to build models of the simpler ternary diagrams. This

may be done easily by the use of artists' modeling clay. Each field is modeled separately in clay of a different color, and the various pieces are fitted into the completed diagram. When finished, the model may be cut horizontally or vertically to obtain the isotherms and isopleths. Another very satisfactory method of making a model of a ternary diagram is by the use of wires to represent all the lines in the diagram, (Fig. 18-4). Cardboard may be used to make the four-phase reaction planes, and colored threads strung horizontally around the wires bounding the three edges of each three-phase region will serve to produce tie-triangles. This kind of model cannot be sectioned, of course, but it has the advantage that the structure can be "seen through" and each field observed *in situ*. Regardless of the method used, it is advisable to make a practice of making sketches of isothermal sections through all space models studied, because this is the form in which the majority of real diagrams are presented. The ultimate objective of working with ternary models is to gain proficiency in the interpretation of isothermal sections.

Interpretation of Complex Ternary Diagrams

Although not always easy to apply, the principles of the interpretation of complex ternary diagrams are themselves simple. As with complex binary systems, the structural changes that take place upon temperature change in an alloy of given composition must be considered one at a time in the order in which they occur, and the influence of the structure as it exists just before each phase change must be taken into account in rationalizing the structural change that follows. Where a multiplicity of phase changes occurs in succession, without equilibrium conditions being approximated in any step, the resulting structures are likely to be very difficult to rationalize.

As a hypothetical example, consider the alloy of composition X in the isothermal sections (of Fig. 18-2) that are presented in Fig. 18-5. If this alloy is heated above its melting point and then allowed to cool, freezing will begin with the primary separation of cored β crystals (Fig. 18-6). At the temperature of the first section, T_1 in Fig. 18-5, primary crystallization is just beginning (Fig. 18-6a). Secondary crystallization of δ is proceeding at T_3 at the expense of both liquid and β , so that in Fig. 18-6b the β has been partly eaten away and is encased in a thick layer of δ . The δ phase disappears at temperature T_4 by decomposition into γ , β , and liquid (Fig. 18-6c). It is to be expected that this reaction, which is at relatively high temperature, will go to completion; the γ phase should appear in places formerly occupied by δ but should share this space with the additional β and liquid that is formed. Freezing of the remaining liquid is completed at T_6 (Fig. 18-6d) by isothermal reaction with β to

stituent showing signs of peritectic attack along its edges, areas of the newly formed ω phase adjacent to the primary β particles, and also smaller particles of a Widmanstätten-precipitated ω within the primary β constituent, a residue of unreacted γ , and also some η in the interdendritic spaces.

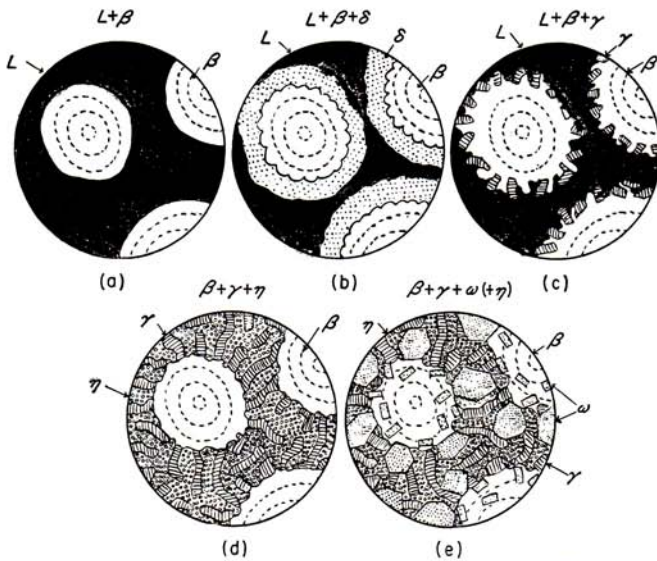


FIG. 18-6. Evolution of the microstructure of alloy X of Fig. 18-5.

Liquidus Projections

A convenient "shorthand" method for representing semiquantitatively the major features of a complex ternary system involves the use of simplified liquidus projections, such as that given in Fig. 18-7. Here only the traces of the valleys of the liquidus (bivariant equilibria) are plotted, and the directions of their slopes toward lower temperature are indicated by arrows inscribed upon the lines. If, in addition, the types of the univariant equilibria (intersections of the lines) are indicated by Roman numerals and the areas of ternariant equilibrium are labeled, a fairly comprehensive representation of the ternary system is obtained. Thus, in Fig. 18-7, point *a* is clearly a eutectic point, $L \rightarrow \alpha + \beta + \gamma$; the Roman numeral I is really not essential here because the sloping of all three valleys toward point *a* identifies it as a ternary eutectic. Points *b* and *c*, being indicated as class II equilibria, evidently represent the reactions $L + \delta \rightarrow \alpha + \beta$ and $L + \eta \rightarrow \alpha + \delta$, respectively. In these cases, as at point *d*, two valleys approach from higher temperature and one proceeds

to lower temperature. But point d is indicated as class I equilibrium. Therefore, it must be one of the solid phases and not the liquid that undergoes eutectic-type decomposition; obviously the θ phase must be unstable below the temperature of d : $\theta \rightarrow \beta + \eta + L$. At point e one valley approaches from higher temperature and two descend to lower temperature. This is a class III equilibrium $L + \beta + \eta \rightarrow \delta$ and represents the maximum temperature of existence of the δ phase.

Further insight into the meaning of this diagram and, at the same time, a check upon the self-consistency of the reactions shown may be had by deriving the plot shown on the opposite page and which is somewhat equivalent to that of Fig. 11-4.

The binary univariant equilibria (without reference to type) are read from the liquidus projection and written in the top line of the foregoing

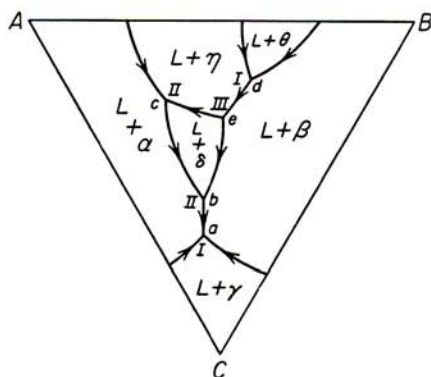
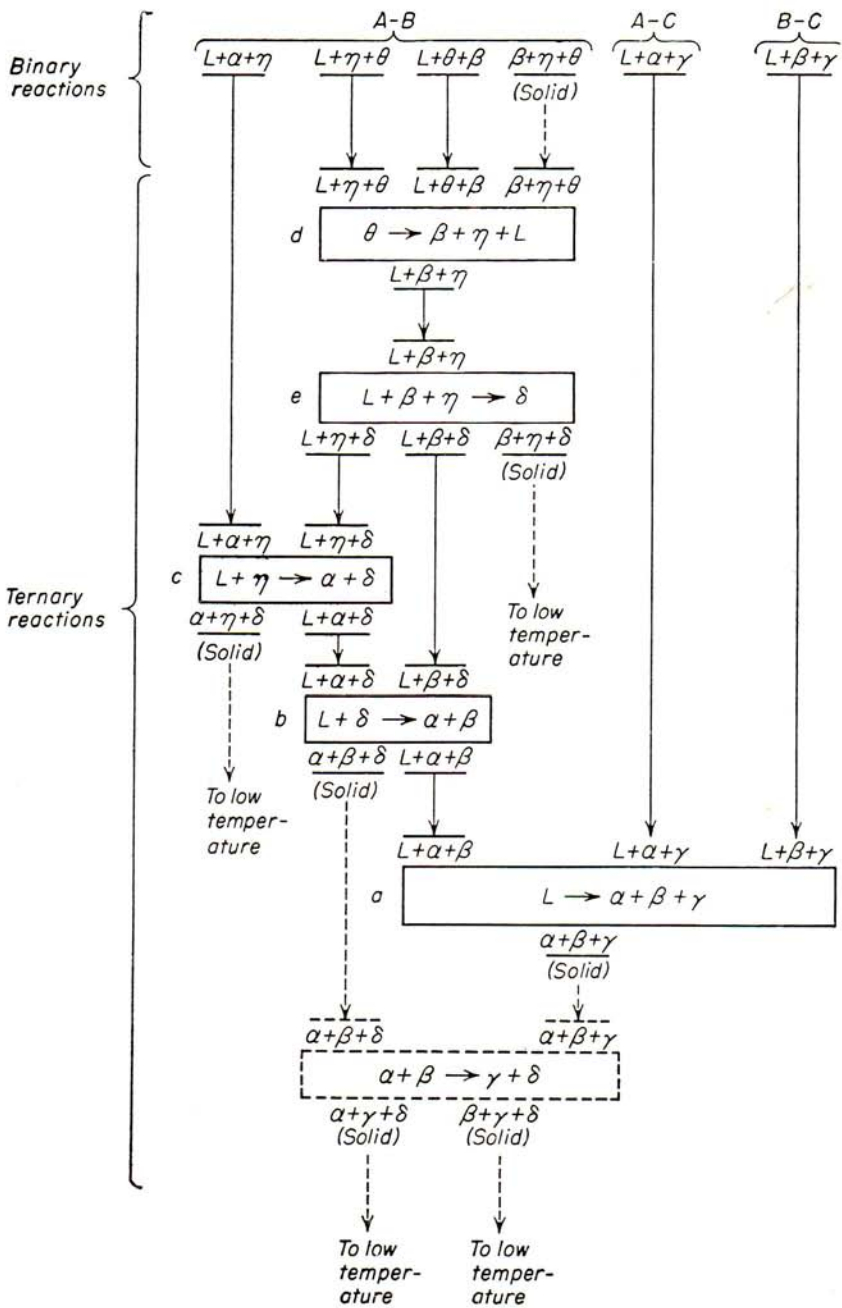


FIG. 18-7. Liquidus projection of a complex ternary system.

plot. In temperature sequence beneath, the ternary univariant equilibria are written and enclosed in "boxes." The four three-phase equilibria associated with each four-phase equilibrium are then written above and below each box, according to the type of four-phase equilibrium concerned. Thus, in the case of $L \rightarrow \alpha + \beta + \gamma$, the three three-phase equilibria involving the liquid phase are written above and the one all-solid three-phase equilibrium below. Next, matching pairs of three-phase groups involving the liquid phase are connected with lines and arrows pointing in the direction of lowering temperature. These represent the temperature spans of the three-phase fields and also the lines and arrows of Fig. 18-7. If the diagram is self-consistent, all three-phase groups involving the liquid phase will thus be paired; only groups of three solid phases will remain unpaired.

Since the projection of Fig. 18-7 represents only the boundaries of the liquid phase, this diagram tells nothing of the relationships obtaining in



those portions of ternary space where all phases are solid. It provides, nevertheless, a basis for speculation concerning solid-state relationships and, taken in conjunction with the binary diagrams, limits the possibilities to some extent. To illustrate, consider the three-phase group $\beta + \eta + \theta$, involving the θ phase, which must disappear at the temperature of d . This group cannot be stable, therefore, below the temperature of point d , and this three-phase equilibrium must occur at higher temperature in the binary system AB . All the other solid-phase groups might be stable at room temperature. Assuming no further solid-state reactions, the room temperature isotherm should include the following three-phase fields: $\beta + \delta + \eta$, $\alpha + \delta + \eta$, $\alpha + \beta + \delta$, and $\alpha + \beta + \gamma$. All two-phase

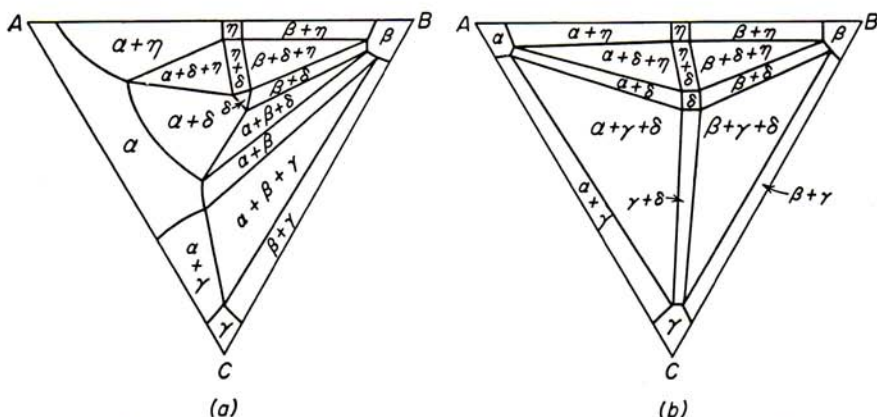


FIG. 18-8. Low-temperature isotherms of the system represented in Fig. 18-7(a) when no solid-state univariant reaction is assumed and (b) when the reaction $\alpha + \beta \rightarrow \gamma + \delta$ is assumed.

pairs that can be made from these three-phase groups will appear as two-phase equilibria, namely, $\beta + \delta$, $\beta + \eta$, $\delta + \eta$, $\alpha + \delta$, $\alpha + \eta$, $\alpha + \beta$, $\alpha + \gamma$, and $\beta + \gamma$. The one-phase fields at room temperature would then be α , β , γ , δ , and η . This would give a room temperature isotherm of the form shown in Fig. 18-8a.

This isotherm may be checked against the binary diagram of the system AC . Unless this binary diagram shows a very broad α field consistent with the isotherm that has been deduced, the evidence is strong that there must be one or more solid-state transformations. For example, the insertion of the transformation $\alpha + \beta \rightarrow \delta + \gamma$ (as indicated by the dashed construction in the foregoing chart) would relieve the necessity for a wide solid-solubility range in the binary system AC (see Fig. 18-8b).

The information given by the liquidus projection can be augmented in several ways. Temperature contours may be shown, and the temperatures

of univariant equilibria indicated. If, in addition, the compositions of the phases participating in the univariant equilibria are listed, the value of the diagram is considerably enhanced. This procedure is illustrated in Fig. 18-9, which is a liquidus projection of the complex diagram shown in Fig. 18-2. It will be seen that down to 600°C the projection gives almost as much information as does the space diagram itself.

Similar projections can, of course, be made of the boundaries of any single-phase field in the space diagram. Of particular usefulness are such projections as that of the γ field in ternary diagrams of the iron-base

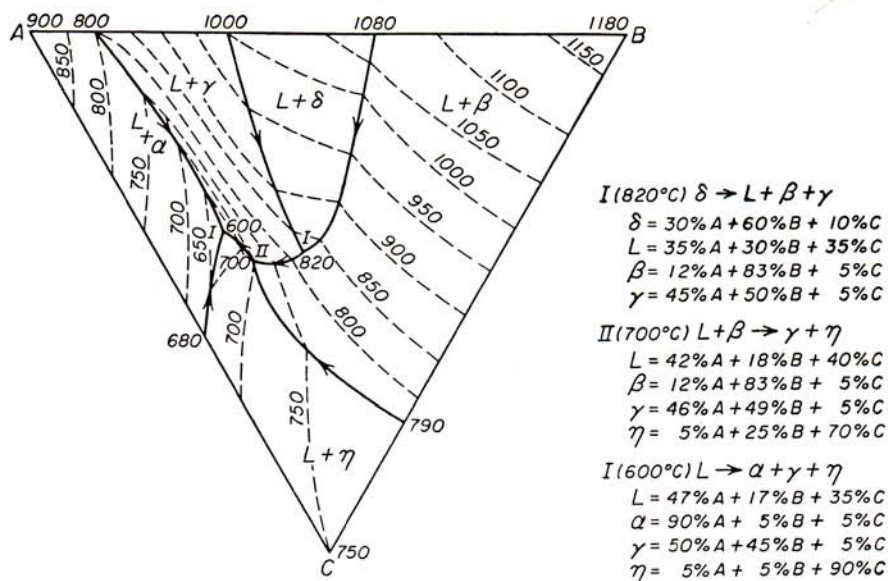


FIG. 18-9. Liquidus projection of the space diagram of Fig. 18-2.

systems. By its use, the pattern of solid-state equilibria can be represented in a simple form. In some cases projections of the solidus have also been employed. These are less satisfactory, however, than liquidus projections and present little additional information.

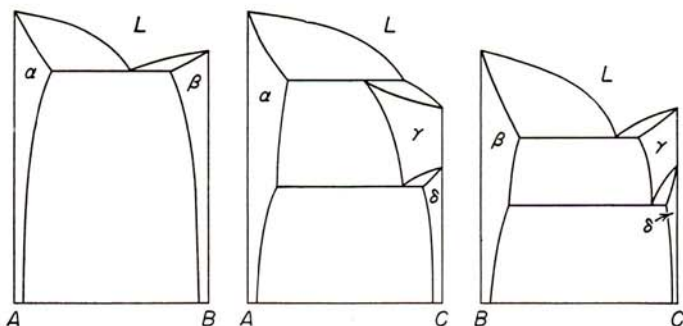
In Chap. 14 a procedure was demonstrated for deducing the course of freezing of specific alloys by the use of the liquidus projection (Fig. 14-10). It will be recalled that the following principles are involved: (1) The liquid composition always changes toward lower temperature, (2) the liquid composition moves away from the compositions of the solid phases that are crystallizing, (3) but one solid phase is crystallizing as long as the liquid composition lies within one of the areas of the liquidus projection (i.e., two-phase region) and (4) two-phase crystallization occurs when the liquid composition is moving down one of the liquidus valleys.

PRACTICE PROBLEMS

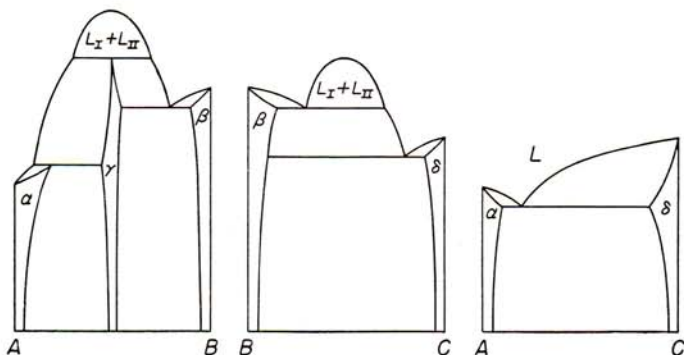
1. A melts at 1000°C , B at 800°C , and C at 600°C ; the system AB has a peritectic reaction at 900°C ; the system AC has a eutectic reaction at 500°C ; the system BC has a eutectic reaction at 400°C ; there is a ternary eutectic reaction at 300°C . Draw the space diagram, and develop isotherms at 950 , 850 , 550 , 450 , 300 , and 250°C . Trace the course of freezing of an alloy containing 10% A and 70% B .

2. In descending order of melting point the components of a ternary system are A , B , and C ; each of the binary systems is of the simple eutectic type; there is a class II four-phase reaction in the ternary space of the diagram; no other isothermal reactions exist in this system. Draw the space diagram, and develop isothermal sections at each temperature level where a new configuration appears.

3. The ternary system ABC of which the three binary diagrams are shown below has two class I four-phase reactions in the space diagram. Complete the space diagram, and develop isothermal sections to show the complete structure of the diagram.



4. The ternary system ABC of which the three binary diagrams are shown below has one class I and two class II four-phase reactions in the space diagram. Complete the space diagram, and develop isothermal sections to show the complete structure of the diagram.



5. From the following vertical sections develop isothermal sections and the space diagram.

